Computer Physics Communications 220 (2017) 230–238

Contents lists available at ScienceDirect

Computer Physics Communications

journal homepage: www.elsevier.com/locate/cpc

On the importance of local orbitals using second energy derivatives for d and f electrons

Ferenc Karsai *, Fabien Tran, Peter Blaha

Institute of Materials Chemistry, Vienna University of Technology, Getreidemarkt 9/165-TC, A-1060, Vienna, Austria

ARTICLE INFO

Article history:
Received 1 March 2017
Received in revised form 7 July 2017
Accepted 11 July 2017
Available online 24 July 2017

Keywords:
LAPW
APW+lo
Local orbitals
WIEN2k
Density functional theory
Lattice constant

ABSTRACT

The all-electron linearized augmented plane wave (LAPW) methods are among the most accurate to solve the Kohn–Sham equations of density functional theory for periodic solids. In the LAPW methods, the unit cell is partitioned into spheres surrounding the atoms, inside which the wave functions are expanded into spherical harmonics, and the interstitial region, where the wave functions are expanded in Fourier series. Recently, Michalicek et al. (2013) reported an analysis of the so-called linearization error, which is inherent to the basis functions inside the spheres, and advocated the use of local orbital basis functions involving the second energy derivative of the radial part (HDLO). In the present work, we report the implementation of such basis functions into the WIEN2k code, and discuss in detail the improvement in terms of accuracy. From our tests, which involve atoms from the whole periodic table, it is concluded that for ground-state properties (e.g., equilibrium volume) the use of HDLO is necessary only for atoms with d or f electrons in the valence and large atomic spheres. For unoccupied states which are not too high above the Fermi energy, HDLO systematically improve the band structure, which may be of importance for the calculation of optical properties.

1. Introduction

The Kohn–Sham (KS) formulation of density functional theory (DFT) [1,2] is the most widely used quantum method for the calculation of geometrical and electronic properties of molecules, clusters, and solids [3,4]. In this method one has to solve the KS equations and this is usually done by expanding the wave functions into some basis set and applying the variational principle. For applications to periodic solids many different methods (basis sets) are available [5], but one of the most accurate schemes is based on the augmented-plane-wave (APW) method of Slater [6].

The APW method is an all-electron method, i.e. it actually treats both, valence and core electrons self-consistently, which is not possible with the very common pseudopotential based methods. In this method, the space is partitioned into spheres centered around the nuclei and an interstitial region [7]. Inside the non-overlapping atomic spheres (often called muffin-tin (MT) spheres) with radius R_{MT} the wave functions are expanded in atomic-like basis functions (radial functions times spherical harmonics), while plane waves are used in the interstitial region, and the two expansions will be matched at the sphere boundary. In the original APW method [6] the radial functions inside spheres $u_{\alpha\ell}(r, E)$ (α is the sphere index and ℓ is the angular momentum) depend on the energy E, which in principle should be set at the (unknown) eigenvalue $\epsilon_{n\mathbf{k}}$ of the wave function $\psi_{n\mathbf{k}}$, and is obtained as numerical solutions of the corresponding radial Schrödinger equation. Requiring $E = \epsilon_{n\mathbf{k}}$ for each wave function leads to a very accurate solution of the KS equation, however, the drawback is that a non-linear eigenvalue problem has to be solved, which is computationally very inefficient.

In order to make APW-based methods more efficient, Andersen introduced the linearized APW method (LAPW) method [8], where $u_{\alpha\ell}(r, E)$ is evaluated at a fixed (linearization) energy $E = E_{\alpha\ell}$ and the radial basis is extended (if we think of it as the second term of a Taylor expansion) by its first energy derivative $\dot{u}_{\alpha\ell}(r, E_{\alpha\ell}) = \partial u_{\alpha\ell}(r, E)/\partial E|_{E=E_{\alpha\ell}}$. However, this energy linearization is accurate only if $E_{\alpha\ell}$ is chosen reasonably close to the true energy E, otherwise the representation of the wave functions, and therefore the results, may be inaccurate [9,10]. The sensitivity of the results on $E_{\alpha\ell}$ is more pronounced for electrons in narrow bands and localized d or f states when using large MT spheres. Typically $E_{\alpha\ell}$ has to be within 0.5–2 Ry of the true eigenvalue depending on angular momentum and the size of the atomic sphere. Ideally, the results for any property like the equilibrium volume or the band structure obtained from an APW-based method should not depend on the size of the atomic sphere, but the corresponding linearization error of the LAPW basis set is one of the main factors for an eventually observed dependency of the results on the size of the MT sphere. Hence, it is an important objective to improve the basis functions

* Corresponding author.
E-mail address: ferenc.karsai@univie.ac.at (F. Karsai).

http://dx.doi.org/10.1016/j.cpc.2017.07.008
0010-4655/

inside the atomic spheres such that the results do not depend on R_{MT}.

Since the original publication of the LAPW method [8], several improvements have been proposed to reduce the linearization error. An overview of the strategies to improve over the LAPW method is available in the work of Michalicek et al. [11], therefore only a brief summary is given below. Early works [12,13] went further in the Taylor expansion of $u_{\alpha\ell}(r, E)$ by using also the second energy derivative $\ddot{u}_{\alpha\ell}(r, E_{\alpha\ell})$. This method turned out to converge much more slowly than the LAPW method (and LAPW converges slower than APW) with respect to the plane wave cut-off $K_{\max}$ [14] due to the additional constraint that not only the wave function (APW) and its first derivative (LAPW) are continuous at the sphere boundary, but also the second derivative, leading to less flexible basis functions.

The original LAPW method has also intrinsic problems with semicore states, which are states at low energy (typically 1–6 Ry below the Fermi energy E_{F}) and fairly, but not completely, localized. The linearization does not allow the simultaneous description of radial functions for two principal quantum numbers of the same angular momentum (e.g., 1*s* and 2*s* in Li). In addition ghost bands may occur [15] when $E_{\alpha\ell}$ is somehow in between the corresponding energies of the two states. Singh [7,14,16] showed that these semicore states can be treated by adding the so-called local orbitals (LO) to the LAPW basis set. A LO is a basis function that is defined only inside the MT sphere and set to zero in the interstitial region (see Section 2.1). Another approach using LO was given by Krasovskii et al. [17–19].

The concept of LO can also be used for different purposes than semicore states. When its expansion energy is carefully selected, LO can reduce the linearization error, and in particular, when we are interested in unoccupied states at sufficiently high energies (e.g., 50 eV above E_{F} for X-ray absorption spectroscopy) one can use LO with an energy parameter set to very high energies describing, e.g., a Li-3*s* function (with two radial nodes). Also, in optimized effective potential (OEP) [20], quasi-particle *GW* [10,21–23] or nuclear magnetic resonance (NMR) [24] calculations, where one needs a good description of the unoccupied states to calculate response functions, multiple LO can be used.

Another very important step was to use local orbitals as a general means to linearize the energy dependency of the radial wave function. In Refs. [25,26], instead of using the energy derivative $\dot{u}_{\alpha\ell}(r, E_{\alpha\ell})$ in the augmented basis functions and requiring continuity in value and slope at the sphere boundary, an APW basis set is used (with a fixed $E = E_{\alpha\ell}$, see Section 2.1), such that only the value of the basis function is made continuous across the sphere when matching to a plane wave. The energy dependency of the basis functions is described by a local orbital with $u_{\alpha\ell}(r, E_{\alpha\ell})$ and its energy derivative $\dot{u}_{\alpha\ell}(r, E_{\alpha\ell})$. This makes the plane wave basis set more flexible and it was shown [26] that with this method the same converged results as with LAPW can be obtained with smaller number of basis functions (about a factor of two), ultimately saving significantly on computer time. Hence we will consider this method, termed as APW+lo (lo in lowercase), as the method of choice in this work.

In recent works, the increase of flexibility of the basis set via LO was further developed. Friedrich et al. [10] employed LO with second energy derivatives $\ddot{u}_{\alpha\ell}(r, E_{\alpha\ell})$ to improve the description of unoccupied states in *GW* calculations. Finally, Michalicek et al. [11] made a careful investigation of possible linearization errors on the results and its elimination using either LO with $\ddot{u}_{\alpha\ell}(r, E_{\alpha\ell})$ or LO defined at high energies (HELO).

In the present work, we report on the implementation of LO using the second energy derivative radial function $\ddot{u}_{\alpha\ell}(r, E_{\alpha\ell})$ into the WIEN2k code [27]. As in Ref. [11], these LO will be termed high derivative LO (HDLO). Our work differs from the work of Michalicek et al. [11] since all our results were obtained using APW+lo as the basic method, while most results shown in Ref. [11] are based on the LAPW basis set. Furthermore, we have made a rather systematic study of the effect of the HDLO on the results in order to figure out for which types of solids and which angular momentum channels it is necessary to add HDLO. HDLO using third or higher energy derivatives of $u_{\alpha\ell}(r, E_{\alpha\ell})$ were not considered, since it was shown that they lead to basically no change in the results that are anyway already converged with second-order HDLO [10]. This paper is organized as follows. A short introduction of the APW+lo method is given in Section 2.1 and in Section 2.2 a detailed derivation of the matrix elements using the HDLO is given. In Section 3, the results are discussed and Section 4 summarizes the main conclusions of this work.

2. Theory

In the APW-type methods, the core and valence electrons are treated differently. Core electrons are defined as having a charge density completely confined within the corresponding atomic sphere. There should be no hybridization (i.e., no band dispersion) and typically their eigenvalues are 6 Ry or more below the Fermi energy. This greatly simplifies the calculation of the core wave functions, since one can simply solve the radial KS (or Dirac) equations inside the MT spheres numerically and does not need any basis-set expansion.

The wave functions of the valence (and semicore) electrons are calculated by solving the KS equations with an APW basis set expansion. As briefly mentioned in Section 1, several linearized APW-based methods and extensions have been proposed. We use by default the APW+lo method for the "chemical" ℓ values (e.g., *s* for Li or $\ell = 0, 1, 2, 3$ for rare-earth and actinide atoms), but LAPW for the higher ("polarization") angular momentum. In Ref. [26], it was shown that it is not necessary to use the (more expensive) APW+lo basis set for the polarization basis functions since the corresponding wave functions, which are more delocalized converge faster with the basis set size. Thus, below we give details of the APW+lo method and its extension. We note that in the rest of this work, the acronyms LAPW and APW+lo implicitly include "+LO" if semicore states are present. In all equations, the spin index is omitted for the sake of simplicity.

2.1. The APW+lo method and its extensions

The basis functions consist of APWs with radial wave functions $u_{\alpha\ell}(r, E_{\alpha\ell})$ defined at a fixed energy $E_{\alpha\ell}$ and local orbitals (lo) [25]. An APW is given by

$$\phi^{\mathrm{APW}}_{\mathbf{k}+\mathbf{K}}(\mathbf{r}) = \begin{cases} \sum_{\ell m} A^{\mathbf{k}+\mathbf{K}}_{\alpha\ell m} u_{\alpha\ell}(r, E_{\alpha\ell}) Y_{\ell m}(\hat{\mathbf{r}}) & \mathbf{r} \in S_\alpha \\ \dfrac{1}{\sqrt{\Omega}} e^{i(\mathbf{k}+\mathbf{K})\cdot\mathbf{r}} & \mathbf{r} \in I, \end{cases} \tag{1}$$

where $\mathbf{K}$ is a reciprocal lattice vector, $\mathbf{k}$ is a point in the first Brillouin zone, $Y_{\ell m}$ are spherical harmonics and $u_{\alpha\ell}$ are solutions of the scalar-relativistic radial KS equation [7] inside the sphere α, as already mentioned in Section 1. The coefficients $A^{\mathbf{k}+\mathbf{K}}_{\alpha\ell m}$ are chosen to match the corresponding plane waves at R_{MT}. The number of APW (or LAPW) basis functions (Eq. (1)) is determined by the cutoff value $K_{\max}$ for the reciprocal lattice vectors $\mathbf{K}$ such that $|\mathbf{k}+\mathbf{K}| \leq K_{\max}$, and very large values corresponding to $R^{\min}_{\mathrm{MT}} K_{\max} = 10$ or 11 were used for the present work ($R^{\min}_{\mathrm{MT}}$ is the smallest atomic radius in the system).

A lo, which is nonzero only inside a MT sphere, is given by

$$\phi^{\mathrm{lo}}_{\alpha\ell m}(\mathbf{r}) = \begin{cases} \left[A^{\mathrm{lo}}_{\alpha\ell m} u_{\alpha\ell}(r, E_{\alpha\ell}) + B^{\mathrm{lo}}_{\alpha\ell m} \dot{u}_{\alpha\ell}(r, E_{\alpha\ell})\right] Y_{\ell m}(\hat{\mathbf{r}}) & \mathbf{r} \in S_\alpha \\ 0 & \mathbf{r} \in I, \end{cases} \tag{2}$$

where $\dot{u}_{\alpha\ell}$ is the first energy derivative of $u_{\alpha\ell}$. The coefficients $A^{\mathrm{lo}}_{\alpha\ell m}$ and $B^{\mathrm{lo}}_{\alpha\ell m}$ are chosen such that $\phi^{\mathrm{lo}}_{\alpha\ell m}$ is zero at R_{MT} and normalized. States that are located far away from E_{F}, such as semicore states (or high-lying empty states), cannot be described accurately by APW+lo. For these states the basis set has to be improved, and this can be done by adding LO containing radial functions $u_{\alpha\ell}$ calculated at the appropriate (e.g., semicore) energy $E^{\mathrm{LO},i}_{\alpha\ell}$:

$$\phi^{\mathrm{LO},i}_{\alpha\ell m}(\mathbf{r}) = \begin{cases} \left[A^{\mathrm{LO},i}_{\alpha\ell m}u_{\alpha\ell}(r,E_{\alpha\ell}) + C^{\mathrm{LO},i}_{\alpha\ell m}u_{\alpha\ell}(r,E^{\mathrm{LO},i}_{\alpha\ell})\right]Y_{\ell m}(\hat{\mathbf{r}}) & \mathbf{r}\in S_\alpha \\ 0 & \mathbf{r}\in I. \end{cases} \tag{3}$$

Note how lo (Eqs. (2)) and LO (Eqs. (3)) differ in their respective second terms.

A clever choice of energy parameters $E_{\alpha\ell}$ in Eqs. (1)–(3) is essential for an accurate APW-based calculation, and WIEN2k has several automatic ways to guarantee an optimal choice in most cases [27], which leads to accurate ground-state properties like the electron density, but also the band gap. The $E_{\alpha\ell}$ of semicore states (actually, of all states whose energy in the free atom is more than 0.5 Ry below the highest occupied atomic orbital, e.g., also C-2*s* or Ar-3*s* states) are selected by searching for two energies E_{bottom} and E_{top}, where the corresponding $u_{\alpha\ell}(R_{MT})$ is zero or has zero slope and taking the average of them. Also, for localized *d* or *f* valence electrons the same procedure is used, but E_{top} is searched only up to 0.5 Ry above E_{F} to insure that the energy parameters are set below E_{F}. The energy parameters of all other valence states are set at 0.2 Ry below E_{F} (or 0.2 Ry above E_{F} if there is a high lying semicore LO to prevent linear dependence). Thus, all our energy parameters are dynamically updated at each iteration of the self-consistent field procedure and not fixed by input. In our experience this is an universally very good choice except when the atomic spheres need to be made very small (e.g., a R_{MT} of 1 Bohr for the C atom due to a short CO or CH bond) or when localized 3*d*/4*f* valence electrons are contributing in a wide energy region.

In Refs. [10,11], Friedrich and co-workers suggested another way to improve the basis set by adding a LO which involves the second energy derivative of $u_{\alpha\ell}$ called HDLO:

$$\phi^{\mathrm{HDLO}}_{\alpha\ell m}(\mathbf{r}) = \begin{cases} \left[A^{\mathrm{HDLO}}_{\alpha\ell m}u_{\alpha\ell}(r,E_{\alpha\ell}) + C^{\mathrm{HDLO}}_{\alpha\ell m}\ddot{u}_{\alpha\ell}(r,E_{\alpha\ell})\right]Y_{\ell m}(\hat{\mathbf{r}}) & \mathbf{r}\in S_\alpha \\ 0 & \mathbf{r}\in I. \end{cases} \tag{4}$$

HDLO were implemented into the FLEUR code [28] and used in the LAPW framework to improve the quality of the basis set. In a few selected cases, they showed that the addition of HDLO to the LAPW basis set could reduce significantly the R_{MT}-dependency of the results for the lattice constant or band structure [10,11]. We have also implemented HDLO into the WIEN2k code and in the following section, details of the Hamiltonian matrix elements which involve HDLO, as implemented into the WIEN2k code, are given.

2.2. Hamiltonian matrix

The Hamiltonian matrix is separated into three components [7]:

$$H = H^{\mathrm{int}} + \sum_\alpha \left(H^{\mathrm{sph}}_\alpha + H^{\mathrm{nsph}}_\alpha\right), \tag{5}$$

where H^{int} is the term from the interstitial region, while H^{sph}_α and H^{nsph}_α are the spherical and non-spherical terms coming from the MT sphere α. H^{sph}_α contains the contributions due to the kinetic-energy operator and the spherical part of the potential V (i.e., the $(\ell, m) = (0, 0)$ term of the $Y_{\ell m}$-expansion of V) and H^{nsph}_α is the contribution from the non-spherical part of V. Detailed formulas for the matrix elements of the Hamiltonian for the LAPW and APW+lo basis sets are already available in the literature [7,29], therefore only the matrix elements involving the HDLO are given below. For the equations in this section, the sphere index α is dropped and $u^i_\ell = u_{\alpha\ell}(r, E^{\mathrm{LO},i}_{\alpha\ell})$.

2.2.1. Spherical contributions to the Hamiltonian matrix

By taking the first and second energy derivatives of

$$\hat{H}^{\mathrm{sph}}|u_\ell\rangle = E_\ell|u_\ell\rangle \tag{6}$$

and neglecting the terms involving a derivative of $\hat{H}^{\mathrm{sph}}$, the expressions for $\hat{H}^{\mathrm{sph}}$ acting on $\dot{u}_\ell$ and $\ddot{u}_\ell$ are given by [10]

$$\hat{H}^{\mathrm{sph}}|\dot{u}_\ell\rangle = |u_\ell\rangle + E_\ell|\dot{u}_\ell\rangle \tag{7}$$

$$\hat{H}^{\mathrm{sph}}|\ddot{u}_\ell\rangle = 2|\dot{u}_\ell\rangle + E_\ell|\ddot{u}_\ell\rangle. \tag{8}$$

Eqs. (7) and (8) are used to derive the expressions for the matrix elements of the spherical part of the Hamiltonian. The functions u_ℓ are normalized ($\langle u_\ell|u_\ell\rangle = 1$) and the first and second derivatives are obtained numerically by finite differences and made orthogonal to u_ℓ ($\langle u_\ell|\dot{u}_\ell\rangle = \langle u_\ell|\ddot{u}_\ell\rangle = 0$). In the case of $\ddot{u}_\ell$, the orthonormalization procedure leads to a linear combination of u_ℓ and $\ddot{u}_\ell$ [10]. Note that in Ref. [10], $\dot{u}_\ell$ and $\ddot{u}_\ell$ are instead obtained as solutions to the inhomogeneous radial Dirac equations. Also, some of the terms in the expressions for the lo–HDLO and LO–HDLO matrix elements are the result of a symmetrization (i.e., average, see Chap. 5.5 in Ref. [7]) in order to ensure that the Hamiltonian is Hermitian.

lo–HDLO:

$$\begin{aligned}\langle\phi^{\mathrm{lo}}_{\ell m}|\hat{H}^{\mathrm{sph}}|\phi^{\mathrm{HDLO}}_{\ell m}\rangle &= E_\ell\left(A^{\mathrm{lo}}_{\ell m}\right)^* A^{\mathrm{HDLO}}_{\ell m} \\ &+ \left(B^{\mathrm{lo}}_{\ell m}\right)^*\left[E_\ell C^{\mathrm{HDLO}}_{\ell m}\langle\dot{u}_\ell|\ddot{u}_\ell\rangle + C^{\mathrm{HDLO}}_{\ell m}\langle\dot{u}_\ell|\dot{u}_\ell\rangle + \frac{1}{2}A^{\mathrm{HDLO}}_{\ell m}\right].\end{aligned} \tag{9}$$

APW–HDLO:

$$\langle\phi^{\mathrm{APW}}_{\mathbf{k}+\mathbf{K}}|\hat{H}^{\mathrm{sph}}|\phi^{\mathrm{HDLO}}_{\ell m}\rangle = E_\ell\left(A^{\mathbf{k}+\mathbf{K}}_{\ell m}\right)^* A^{\mathrm{HDLO}}_{\ell m}. \tag{10}$$

LO–HDLO:

$$\begin{aligned}\langle\phi^{\mathrm{LO},i}_{\ell m}|\hat{H}^{\mathrm{sph}}|\phi^{\mathrm{HDLO}}_{\ell m}\rangle &= E_\ell\left(A^{\mathrm{LO},i}_{\ell m}\right)^* A^{\mathrm{HDLO}}_{\ell m} \\ &+ \left(C^{\mathrm{LO},i}_{\ell m}\right)^*\frac{1}{2}\left(E_\ell + E^{\mathrm{LO},i}_\ell\right)\left[A^{\mathrm{HDLO}}_{\ell m}\langle u^i_\ell|u_\ell\rangle + C^{\mathrm{HDLO}}_{\ell m}\langle u^i_\ell|\ddot{u}_\ell\rangle\right] \\ &+ \left(C^{\mathrm{LO},i}_{\ell m}\right)^* C^{\mathrm{HDLO}}_{\ell m}\langle u^i_\ell|\dot{u}_\ell\rangle.\end{aligned} \tag{11}$$

HDLO–HDLO:

$$\begin{aligned}\langle\phi^{\mathrm{HDLO}}_{\ell m}|\hat{H}^{\mathrm{sph}}|\phi^{\mathrm{HDLO}}_{\ell m}\rangle &= E_\ell\left(\left|A^{\mathrm{HDLO}}_{\ell m}\right|^2 + \left|C^{\mathrm{HDLO}}_{\ell m}\right|^2\langle\ddot{u}_\ell|\ddot{u}_\ell\rangle\right) \\ &+ 2\left|C^{\mathrm{HDLO}}_{\ell m}\right|^2\langle\dot{u}_\ell|\ddot{u}_\ell\rangle.\end{aligned} \tag{12}$$

2.2.2. Non-spherical contributions to the Hamilton matrix

The contributions to the Hamilton matrix of the non-spherical part $\hat{H}^{\mathrm{nsph}}$ are given by

$$\langle\phi_i|\hat{H}^{\mathrm{nsph}}|\phi_j\rangle = \sum_{p,q}\sum_{\ell=0}^{\ell^{\mathrm{nsph}}_{\mathrm{max}}}\sum_{m=-\ell}^{\ell}\sum_{\ell'=0}^{\ell^{\mathrm{nsph}}_{\mathrm{max}}}\sum_{m'=-\ell'}^{\ell'} D^{ip}_{\ell m}t^{v^p_\ell w^q_{\ell'}}_{\ell m\ell' m'}D^{jq}_{\ell' m'}, \tag{13}$$

where $D^{ip}_{\ell m}$ represent the coefficients of the basis functions ϕ_i (and similar for ϕ_j), which are equally defined for APW+lo and all kinds of local orbitals, $t^{v^p_\ell w^q_{\ell'}}_{\ell m\ell' m'}$ are integrals defined as

$$t^{v^p_\ell w^q_{\ell'}}_{\ell m\ell' m'} = \sum_{\ell''=0}^{\ell^{\mathrm{nsph}}_{\mathrm{max}}}\sum_{m=-\ell''}^{\ell''} G^{mm''m'}_{\ell\ell''\ell'}\int_0^{R_{\mathrm{MT}}} r^2 v^p_\ell(r)V_{\ell'' m''}(r)w^q_{\ell'}(r)dr, \tag{14}$$

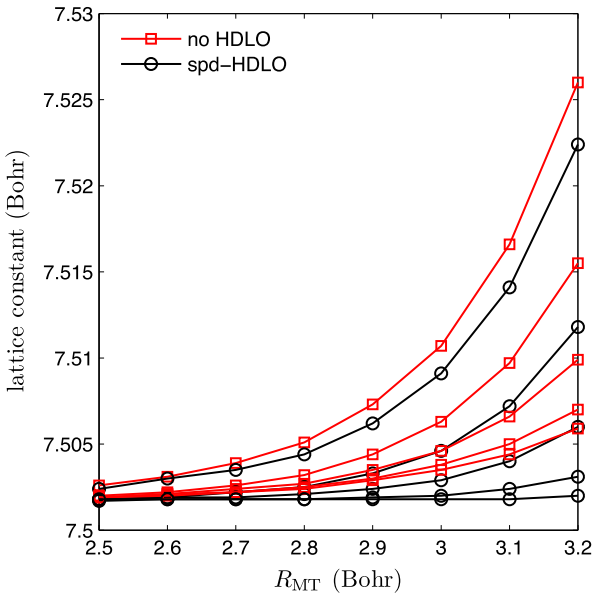

Fig. 1. R_{MT}-dependency of the equilibrium lattice constant of CsCl with or without *spd*-HDLO added at the Cl atom, and for different values of ℓ_{max}^{nsph}. The curves from top to bottom correspond to $\ell_{max}^{nsph} = \{4, 5, 6, 7, 8\}$, respectively. R_{MT} was varied for both atoms at the same time.

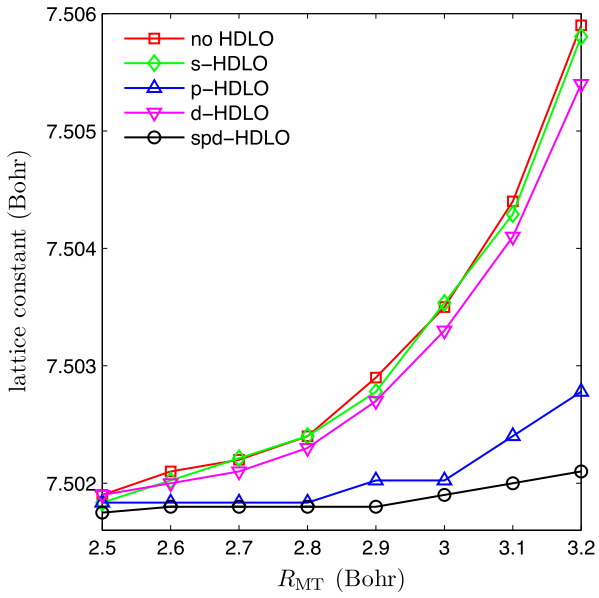

Fig. 2. R_{MT}-dependency of the equilibrium lattice constant of CsCl with or without HDLO added at the Cl atom for different angular momenta ℓ. R_{MT} was varied for both atoms at the same time.

where v_ℓ^p and $w_{\ell'}^q$ are the radial functions u_ℓ, $\dot{u}_\ell$, $\ddot{u}_\ell$ or u_ℓ^i, and $G_{\ell\ell''\ell'}^{mm''m'}$ are Gaunt coefficients:

$$G_{\ell\ell''\ell'}^{mm''m'} = \int_0^{2\pi}\int_0^{\pi} Y_{\ell m}^*(\theta,\phi)Y_{\ell'' m''}(\theta,\phi)Y_{\ell' m'}(\theta,\phi)\sin(\theta)d\theta d\phi. \tag{15}$$

Since the triple sum over ℓ, ℓ' and ℓ'' in Eq. (13) can get quite involved, a careful choice for ℓ_{max}^{nsph}, which should be smaller than ℓ_{max} (the maximum angular momentum for the spherical part of the Hamiltonian), is important.

3. Results

We start by mentioning that in the course of our investigations, we observed that for atomic sphere radii R_{MT} larger than 2.2–2.5 Bohr, our default cutoff $\ell_{max}^{nsph} = 4$ for the $Y_{\ell m}$-expansion of the orbitals in the calculation of the non-spherical part of the Hamiltonian (see Eq. (13)) is not converged. (By default, ℓ_{max} is set to 10, which is a very well converged value.) Actually, by increasing ℓ_{max}^{nsph}, a rather large portion of the R_{MT}-dependency of the results could be removed in most cases. Fig. 1 shows the example of CsCl, where we can see that if a R_{MT} larger than 3 Bohr is used for the calculations, then convergence for the equilibrium lattice constant is reached with $\ell_{max}^{nsph} = 7$, while with the default $\ell_{max}^{nsph} = 4$ the lattice constant is too large by a non-negligible amount. We have observed a similar behavior for all other systems, except the alkaline and alkaline-earth atoms that are much more spherical and for which $\ell_{max}^{nsph} = 4$ is already enough. From now on, all results that are shown were obtained with $\ell_{max}^{nsph} = 8$, such that the observed R_{MT}-dependencies are only due to an incomplete basis set.

We have investigated the effect of adding HDLO to the APW+lo basis set for many solids (Na, K, C, Si, Sn, Cu, Zn, Ag, Cd, Au, La, Ce, Po, Th, KCl, MgO, CaO, CsCl, etc.), which were chosen such that atoms from all parts of the periodic table are represented. Among them, a few were selected as representative examples and are listed in Table 1 along with their structural parameters, the states that were treated in the core, and the LO that were added for the semicore states. The c/a ratio of the hexagonal solids was kept constant during the volume optimization. The convergence parameters which are not related to the basis set, like the size of the **k**-mesh or the cutoff for the expansion of the density and potential, were chosen to be very well converged. Concerning the exchange–correlation functional, the local density approximation [30] was used. As mentioned in Section 1, the results of a calculation may depend on the size of the MT sphere, and in order to illustrate this problem we will consider the equilibrium lattice constant, the electronic structure and the electric-field gradient (EFG). As in Ref. [11], we will show that a R_{MT}-dependency of the results, if present, can be eliminated to a large degree by adding HDLO to the basis set.

Let us start the discussion with the R_{MT}-dependency of the lattice parameters. We first note that even with the default APW+lo basis set the dependency of the results on R_{MT} is very weak for elements that have only *s* valence electrons. For the alkaline and alkaline-earth metals, i.e., the *s* block of the periodic table (Na, K, Ca and Cs were considered), the equilibrium lattice constant is the same (variation of 0.001 Bohr at most) in the whole range of R_{MT} that we have considered (R_{MT} between roughly 1.5 and 3 Bohr). This was to be expected since the valence *s*-electrons of these elements are very diffuse with maxima far outside the atomic spheres and a rather weak energy dependency of their radial wave functions inside the atomic spheres. Thus, for these systems the standard APW+lo basis set (with the WIEN2k choice of energy parameters $E_{\alpha\ell}$ as outlined above) is already good enough such that it is not necessary to add HDLO.

For solids containing atoms of the *p* block (we considered Al, Po, CsCl and a few others), we found that the variation of the equilibrium lattice constant with R_{MT} is also rather weak and typically smaller than 0.005 Bohr. Although our test set is limited, this conclusion should be of rather general validity among the *p* block systems. As an example, Fig. 2 shows the lattice constant of CsCl as a function of R_{MT}, which was set to be the same for both the Cs and Cl atoms. With the APW+lo basis set without HDLO, the lattice constant varies from 7.502 Bohr with the smallest R_{MT} (2.5 Bohr) to 7.506 Bohr with the largest R_{MT} (3.2 Bohr). Let us mention that by varying the sphere size for one atom, while keeping fixed the other

Table 1
List of solids considered in this work. Also shown are the space group, c/a ratio for hexagonal solids, electronic states treated in the core and the LO (within the APW+lo scheme) added for semicore states.

Solid	Space group	c/a	Core states	Semicore LO
Ar	$Fm\bar{3}m$		[Ne]	3*s*
Cd	$P6_3/mmc$	1.8858	[Ar]3*d*	4*s*, 4*p*
Gd	$P6_3/mmc$	1.5904	[Kr]4*d*	5*s*, 5*p*
Ce	$Fm\bar{3}m$		[Kr]4*d*	5*s*, 5*p*
KCl	$Fm\bar{3}m$		K: [Ne]; Cl: [Ne]	K: 3*s*, 3*p*; Cl: 3*s*
CsCl	$Pm\bar{3}m$		Cs: [Kr]; Cl: [Ne]	Cs: 4*d*, 5*s*, 5*p*; Cl: 3*s*

one, we could see that the R_{MT}-dependency of the lattice constant is mostly due to the Cl atom. As shown in Fig. 2, adding HDLO to the basis set for the Cl atom makes the curve nearly constant at 7.502 Bohr. As expected, the effect comes mainly from the addition of a HDLO at $\ell = 1$, i.e., the linearization error with APW+lo was the largest for the Cl 3*p* electrons. Adding a HDLO also at $\ell = 2$ reduces further the variation of the lattice constant with R_{MT}. We note that for KCl (rock-salt structure), Ref. [11] reports a difference of ~ 0.05 Bohr between the lattice constant calculated with R_{MT} of 2.1 and 2.8 Bohr by using the LAPW basis set (without HDLO). This is ten times larger than what we obtained for KCl with the APW+lo basis set without HDLO (results not shown). We have checked that this difference with respect to our results is not due to a different choice of basis set (LAPW versus APW+lo), but the most plausible explanation is related to the different strategies used in the two codes for choosing the energy parameters $E_{\alpha\ell}$ and our automatic procedure seems (at least in this case) to be more efficient.

Next, we turn to the transition metals for which the R_{MT}-dependency of the lattice constants is expected to be larger than for the *s* and *p* solids considered so far, because the *d* wave functions are much more localized around the atoms and thus show a much larger energy dependency inside the atomic spheres. This also leads to a greater sensitivity of the results on the chosen energy parameter $E_{\alpha\ell}$ and an optimal adjustment of $E_{\alpha\ell}$ is more difficult to achieve. We show in Fig. 3 the large relativistic component of $u_{\alpha\ell}$ (multiplied by r) for the 4*d* state in Cd evaluated at values of $E_{\alpha\ell}$ ranging from -1 to 1 Ry around the Fermi energy. At this scale, a visible change in the shape of $u_{\alpha\ell}$ starts already at 1 Bohr and increases monotonously and becomes very non-linear for distances above 2 Bohr. Therefore, some linearization error should be clearly expected for R_{MT} above 2 Bohr and this is what we can see in Fig. 4. Without HDLO, the change in the lattice constant with respect to R_{MT} (varied between 1.9 and 2.6 Bohr) is approximately 0.01 Bohr. This can be ascribed entirely to the linearization error for the *d* electrons since adding a HDLO for $\ell = 2$ leads to a practically constant value of the lattice constant (5.492 Bohr).

The R_{MT}-dependency is also large for solids with valence *f* states as shown in Figs. 5 and 6 for Ce and Gd, respectively. As already discussed in Ref. [11], Ce is an extreme case since the lattice constant varies from 8.54 Bohr (at $R_{MT} = 2.1$ Bohr) to 8.66 Bohr (at $R_{MT} = 3.0$ Bohr). This is a variation which is one order of magnitude larger than for the cases considered up to now. The use of a HDLO at $\ell = 3$ to improve the description of the 4*f* states removes 90% of the linearization error, while the rest can be mostly eliminated by adding a HDLO at $\ell = 2$ (5*d* states). We note that, as shown in Fig. 5, the lattice constant from Ref. [11] calculated with the LAPW+HDLO basis set agrees very well with our value. The case of hexagonal Gd (Fig. 6) is not so dramatic as for Ce since the lattice constants at the smallest (1.8 Bohr) and largest (3.0 Bohr) R_{MT} differ by about 0.02 Bohr, but this is still a quite large discrepancy. Again, adding HDLO at angular momenta $\ell = 2$ and $\ell = 3$ makes the curve flat at 6.597 Bohr. We mention that the same was observed for the other *f* systems that we investigated (La and Th).

For each test case that they considered, Michalicek et al. [11] showed that the R_{MT}-dependency can also be removed by using HELO. They concluded that the results with HDLO can be (nearly) reproduced by using two HELO (i.e., two sets of HELO of successive principal quantum number for a given ℓ), while the use of only one HELO was not sufficient. For a few cases we also investigated the

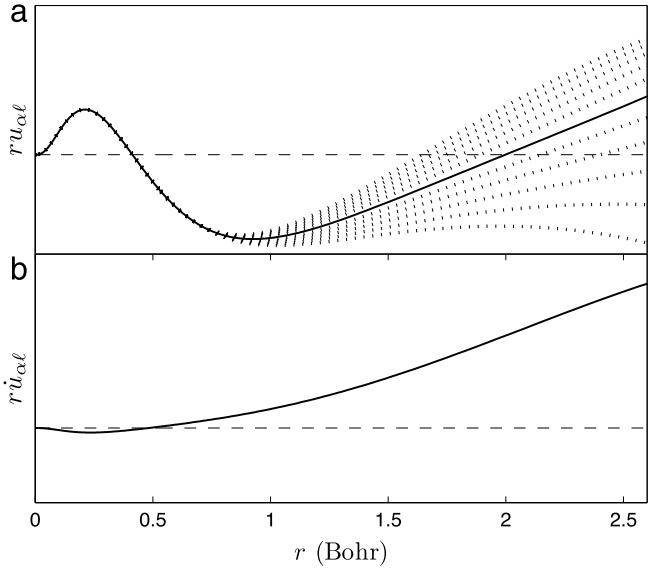

Fig. 3. (a) Large relativistic component of $ru_{\alpha\ell}$ in Cd for $\ell = 2$ at various values of $E_{\alpha\ell}$ that was varied with step of 0.2 Ry from -1 Ry (lower curve) to 1 Ry (upper curve) around the Fermi energy E_F. The solid curve corresponds to $E_{\alpha\ell} = E_F$. (b) $r\dot{u}_{\alpha\ell}$ for $E_{\alpha\ell} = E_F$. In the two panels, the horizontal dashed line represents a value of zero.

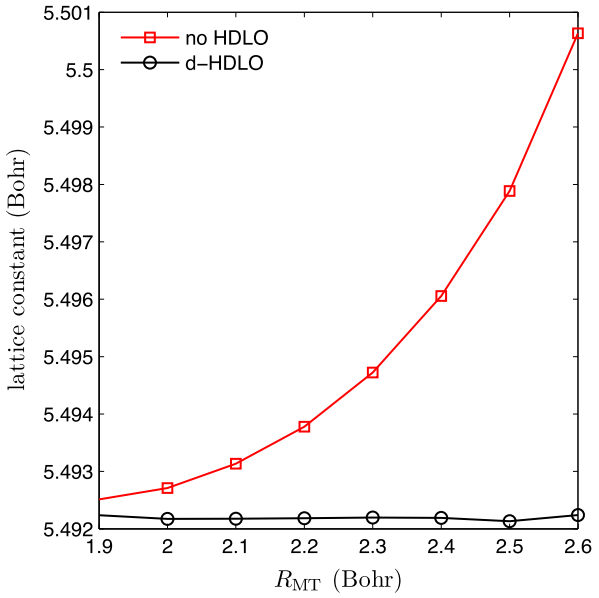

Fig. 4. R_{MT}-dependency of the equilibrium lattice constant a (c/a is kept fixed, see Table 1) in Cd.

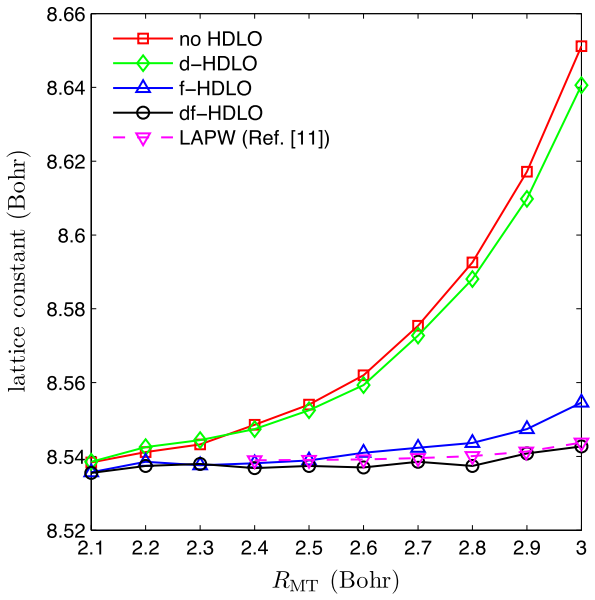

Fig. 5. R_{MT}-dependency of the equilibrium lattice constant in Ce. For comparison, the results from Ref. [11] using the LAPW method with HDLO are also shown.

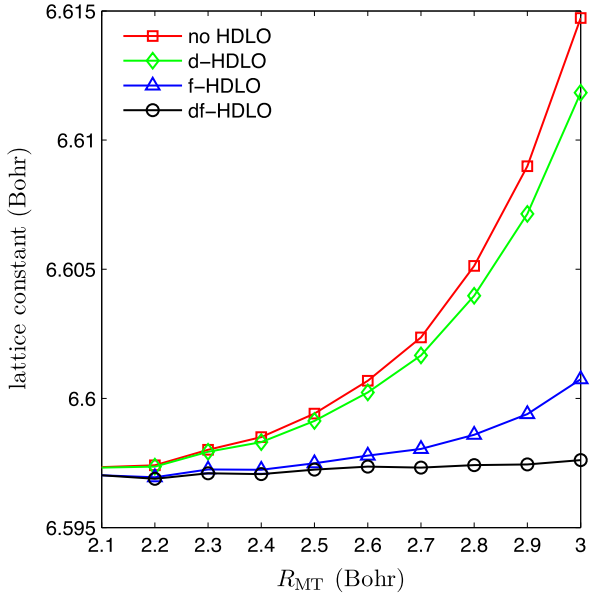

Fig. 6. R_{MT}-dependency of the equilibrium lattice constant a (c/a is kept fixed, see Table 1) in Gd.

use of HELO and found that one set of HELO, if set at the appropriate energy, is sufficient to reduce the R_{MT}-dependency the same way as HDLO do. For Gd, for instance, exactly the same curves as in Fig. 6 can be obtained by adding one HELO for the d, f or both d and f angular momentum at energies above the Fermi energy. From the practical point of view, HDLO are eventually preferable since their energy parameters $E_{\alpha\ell}$ are set at the same value as for the APW+lo basis functions, while the use of HELO requires choosing new energy parameters $E_{\alpha\ell}^{\mathrm{LO},i}$. In order to avoid problems like ghost bands, $E_{\alpha\ell}^{\mathrm{LO},i}$ have to be set at energies that are well separated from the valence bands, i.e., at least ∼0.5 Ry above the Fermi energy. On the other hand, $E_{\alpha\ell}^{\mathrm{LO},i}$ should not be set too high, otherwise the HELO will be of little use to improve the description of the occupied orbitals. However, as shown below, only HELO can help to improve the description of very high-lying unoccupied states.

Let us now consider the electronic structure and Fig. 7 which shows, for the largest R_{MT}, the changes in the band structures when adding HDLO to the APW+lo basis set. We observe that in general there is no visible effect for the occupied and the first unoccupied bands, but HDLO clearly affect the position and shape of the bands starting from about 10 eV above the Fermi energy. The linearization error can lead to bands which are shifted to higher energy by as much as 1 eV in this energy range. Similar as for the lattice constant, the band structures calculated with large R_{MT} and HDLO correspond very well to those with small R_{MT} (with or without HDLO). Note that such observations occur in all compounds and therefore HDLO are useful to correct the linearization errors in unoccupied bands for any kind of systems. However, it is important to remember that the linearization energies in APW+lo+HDLO calculations are set in the occupied part of the spectrum, therefore one should not expect an accurate representation of very high-lying unoccupied states. For an accurate treatment of all unoccupied states, additional LO have to be set at the corresponding energies, and this is what has been done for the calculation of the response function in the OEP [20] and *GW* [10,21–23] methods, and for the calculation of the NMR chemical shift [24].

However, it is rather obvious that for states that are further high in energy, HDLO should not be efficient anymore and only HELO can be helpful for an accurate calculation of such very high-lying states. Fig. 8 compares the band structures of Gd calculated with HDLO and HELO. By setting the energy parameters of the HELO above 30 eV (for s, p, d and f angular momentum in the present case of Gd), we can see that states that are above this energy are described more accurately since they are lower in energy (using this criterion in this context) than in the case with HDLO. Thus, depending on the energy range of unoccupied states that is required for the calculation of a given property (e.g., X-ray absorption or response function), it may be necessary, in addition to HDLO, to add HELO to the basis set with energy parameters set at these high energies.

We note that Michalicek et al. [11] reported a reduction of the band gap in the rare-gas solid Ar of nearly 2 eV (at Γ) when a HDLO is added to their LAPW basis set. In our case the reduction of the band gap is one order of magnitude smaller (∼0.2 eV). The main reason should be due to our basis set for Ar which contains by default one more semicore LO (for 3s states, see Table 1) compared to the basis set used in Ref. [11]. However, our scheme for choosing the energy parameters $E_{\alpha\ell}$ may also play a role.

Finally, we also demonstrate that details of the electron density may also be affected by the basis set and we show this on a very sensitive quantity, namely the EFG V_{zz}, which can be obtained from an integral of the charge density ρ as [31]

$$V_{zz} \propto \int \frac{\rho(\mathbf{r})}{r^3} Y_{20}(\hat{\mathbf{r}}) d^3r. \tag{16}$$

Fig. 9 shows the EFG in Cd as function of R_{MT}, where we can see that without HDLO the EFG varies rather strongly from 8.06×10^{21} V/m^2 at $R_{MT} = 1.9$ Bohr to 8.27×10^{21} V/m^2 at $R_{MT} = 2.6$ Bohr, while the use of a d-HDLO leads to results which show a much weaker variation with the R_{MT}.

All the results that have been presented so far have shown that HDLO are very efficient at eliminating linearization errors that may be present in APW+lo calculations. The use of HDLO is strongly recommended for calculations with large MT spheres (let us say larger than 2.3–2.5 Bohr depending on the case) and in particular for atoms with d or f valence electrons. However, we should mention that we also observed that it is not possible to add blindly HDLO at all angular momenta ℓ since this may lead to technical problems during the self-consistent field procedure, e.g., linear dependency or ghost bands. Fortunately, such problems seem to occur only for states which anyway do not require HDLO

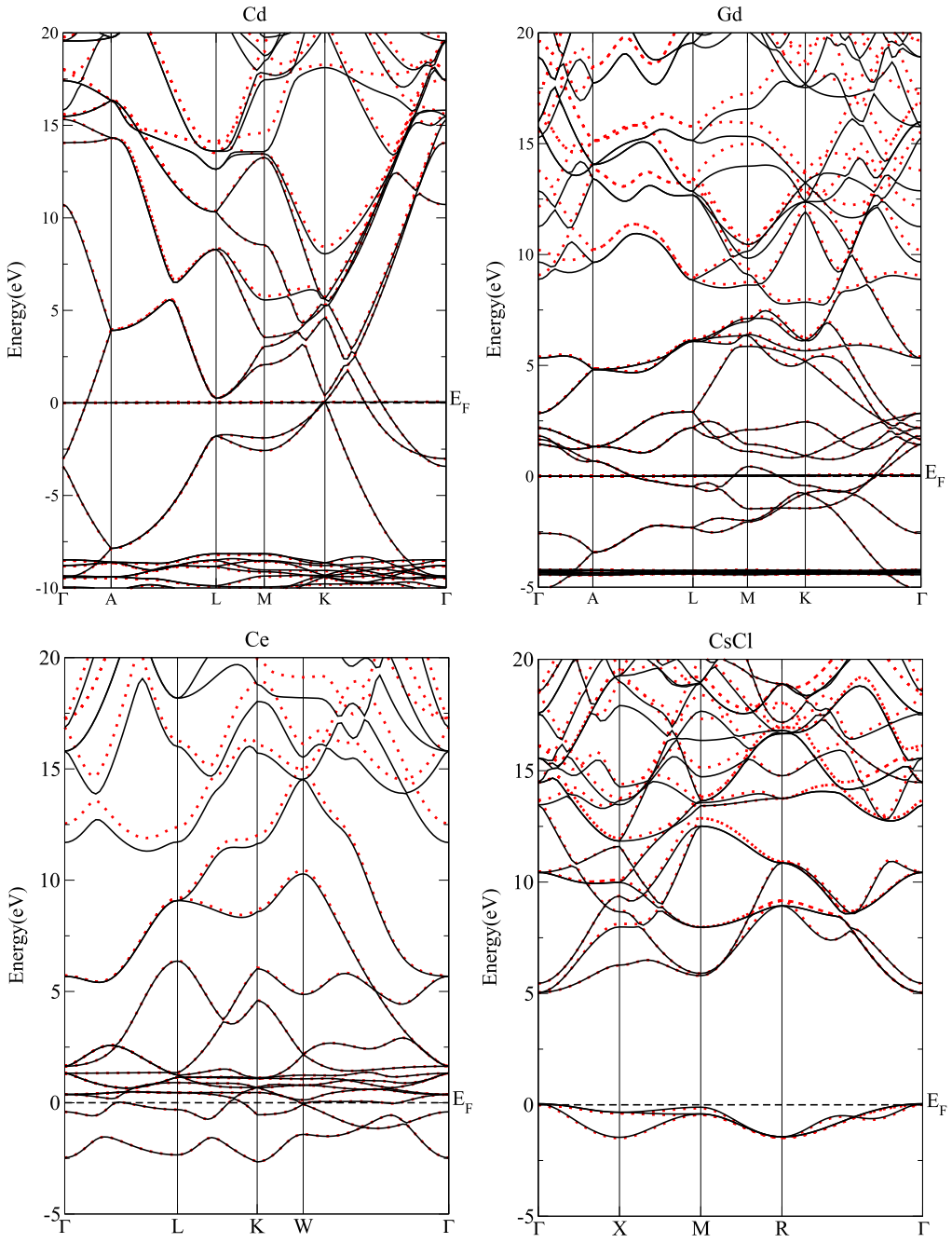

Fig. 7. Band structures for large R_{MT}. Band structures without HDLO and with HDLO are plotted with red (dotted) and black (solid) lines, respectively. R_{MT} of 2.6, 3.0, 3.0 and 3.2 Bohr were used for Cd, Gd, Ce and CsCl, respectively. Lattice constants of 5.474, 6.584, 8.525 and 7.502 Bohr were used for Cd, Gd, Ce and CsCl, respectively. The band structure of Gd is for spin up.

since the energy dependency of their radial wave functions is very small and the APW+lo basis set is already complete.

A typical problem can arise when MT spheres are (or have to be) chosen very small, and to illustrate this, we show the example of the CO molecule (placed in a large unit cell), where the equilibrium distance between the C and O atoms is so small (about 2.1 Bohr) that typically a R_{MT} of 0.9 Bohr for the C atom would be used. Calculations with such small MT spheres work fine as long as the regular APW+lo basis set without HDLO is used. The eigenvalues of the molecular orbitals vary by about 2 Ry from the lowest occupied MO to the lowest unoccupied orbital and thus one may worry that the linearization may not be completely accurate over such a large energy window. However, when adding HDLO for the C-2*s* states, a ghost band at low energy appears in the molecular orbital diagram. In order to understand why it occurs, we show in Fig. 10 for a single isolated C atom, the components of a 2*s*-HDLO (multiplied by r) evaluated at an energy of 0.2 Ry below E_F. Since $\ddot{u}_{\alpha\ell}$ is very small at the sphere boundary compared to $u_{\alpha\ell}$ the coefficient $A^{HDLO}_{\alpha\ell m}$ in Eq. (4) has to be chosen very small so that the combination of $u_{\alpha\ell}$ and $\ddot{u}_{\alpha\ell}$ is zero at the sphere boundary as required for a HDLO. For a sphere radius of 0.9 Bohr it can be clearly seen (Fig. 10(c)) that the linear combination of $u_{\alpha\ell}$ and $\ddot{u}_{\alpha\ell}$ looks like a "bad" 1*s* function, as it has a node close to the boundary of the MT sphere instead of going smoothly to zero. Adding such a HDLO to the basis set thus provides a poor C-1*s* basis function and consequently the corresponding "1*s*" eigenvalue is much too high and appears as a ghost band

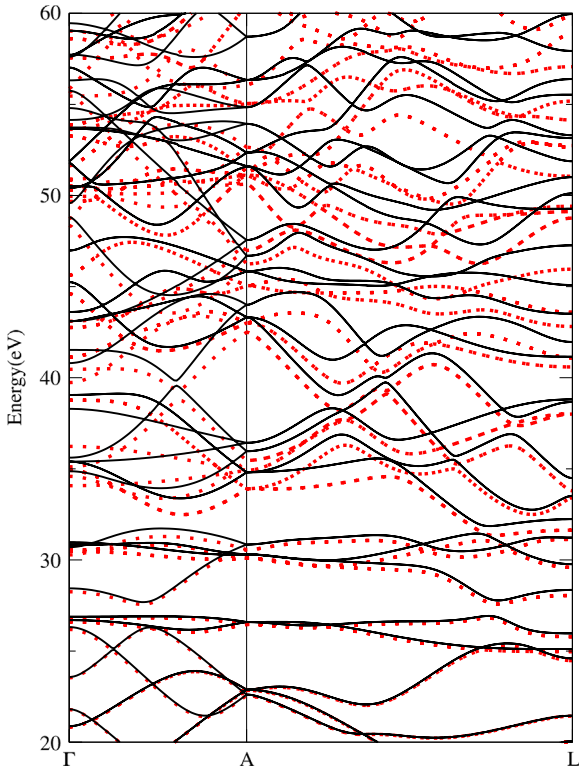

Fig. 8. Spin-up band structure of Gd calculated with HDLO (black solid line) or with HELO (red dotted line). The calculations were done with $R_{\mathrm{MT}} = 3.0$ Bohr and at the lattice constant of 6.584 Bohr.

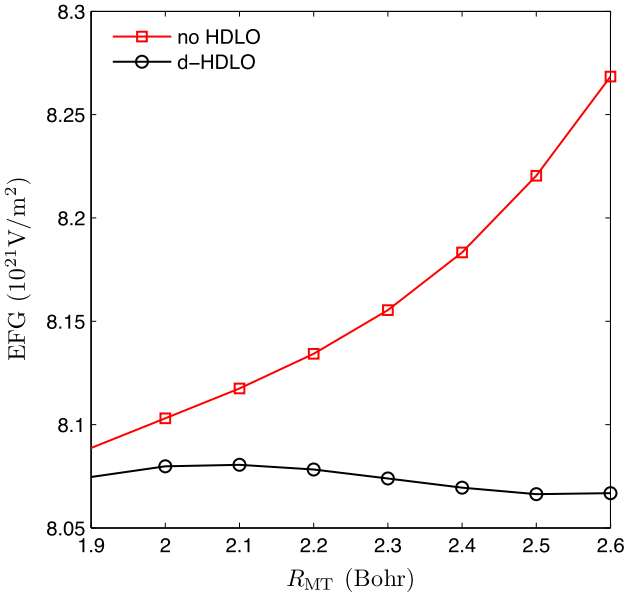

Fig. 9. R_{MT}-dependency of the EFG in Cd. The calculations were done at the lattice constants $a = 5.629$ Bohr and $c = 10.616$ Bohr.

in the eigenvalue spectrum. This behavior happens only for very small R_{MT} (Fig. 11). For a larger MT sphere around the C atom, the local orbital is very different and looks like a 2*s* basis function, which is used in the variational calculation to provide an excellent description of the energy dependency of the 2*s* functions and no ghost bands appear in the calculation. It should be mentioned that the tendency to get ghostbands is reduced with the LAPW+HDLO method (compared to APW+lo+HDLO), but can still occur.

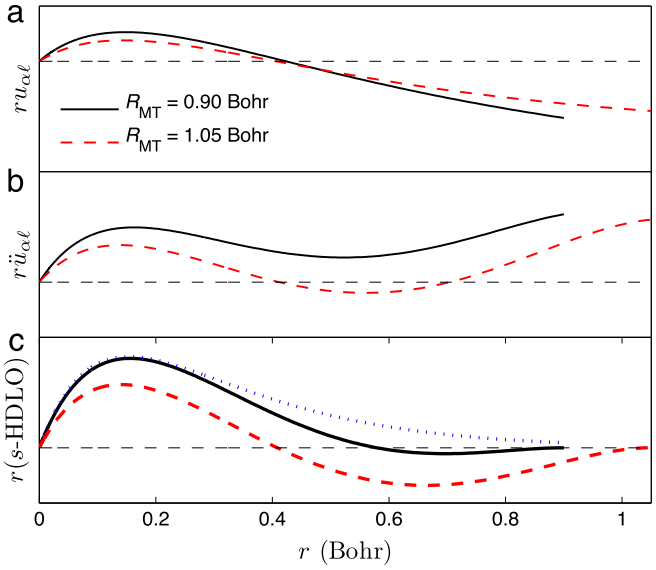

Fig. 10. Radial components of a HDLO with $\ell = 0$ for a single C atom placed in a large box. (a), (b) and (c) show $ru_{\alpha\ell}$, $r\ddot{u}_{\alpha\ell}$ and their linear combination $A^{\mathrm{HDLO}}_{\alpha\ell m} ru_{\alpha\ell} + C^{\mathrm{HDLO}}_{\alpha\ell m} r\ddot{u}_{\alpha\ell}$, respectively. The matching coefficients $A^{\mathrm{HDLO}}_{\alpha\ell m} = 0.00299$ for $R_{\mathrm{MT}} = 0.9$ Bohr and $A^{\mathrm{HDLO}}_{\alpha\ell m} = 0.00314$ for $R_{\mathrm{MT}} = 1.05$ Bohr were determined by requiring that the HDLO is zero at the MT sphere boundary ($C^{\mathrm{HDLO}}_{\alpha\ell m}$ was set to 1). In the three panels, the horizontal dashed line represents a value of zero. The blue dotted line in the bottom panel shows the 1*s* function obtained from a fully relativistic calculation with its maximum scaled to the maximum of the curve with $R_{\mathrm{MT}} = 0.90$ Bohr.

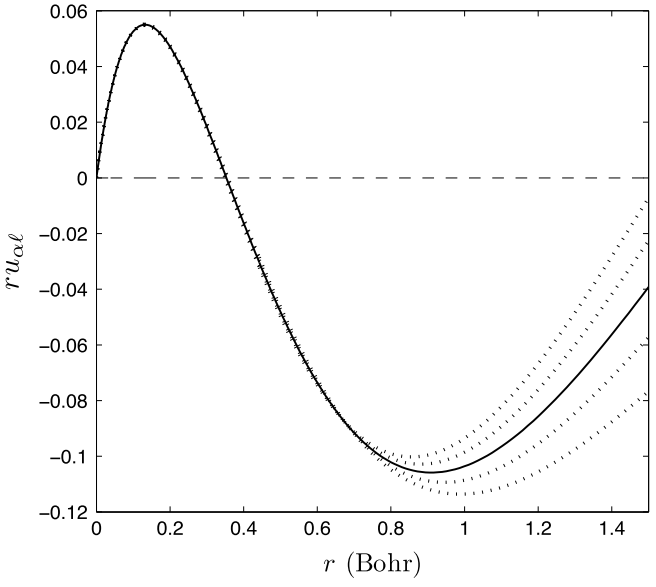

Fig. 11. Large relativistic component of $ru_{\alpha\ell}$ for $\ell = 0$ for a single C atom in a large box. Each curve corresponds to a value of $E_{\alpha\ell}$ that was varied with step of 0.5 Ry from −1 Ry (lower curve) to 1 Ry (upper curve) around the Fermi energy E_{F}. The solid curve corresponds to $E_{\alpha\ell} = E_{\mathrm{F}}$.

4. Summary

In this work, we have investigated in detail the ability of HDLO to improve the quality of the basis set in the framework of the APW+lo method. An improvement of the APW+lo basis set is particularly important for calculations with large MT spheres for atoms containing *d* or *f* electrons in the valence, since the linearization error can be particularly large in such cases. Actually, the use

of large MT spheres has two advantages: faster calculations since a smaller cutoff K_{max} for the expansion of the wave functions can be used and reduced leakage of the core density outside the MT spheres.

A short summary of our observations is the following. For the equilibrium geometry, a ground-state property, the effect of the linearization error is very small for atoms of the *s* and *p* blocks of the periodic table (basically absent for *s* systems), such that the use of HDLO is not really necessary even for very large MT spheres. Two calculations with very different MT sphere sizes lead to lattice constants which differ by at most 0.005 Bohr, which is small and usually unimportant for practical applications. For atoms containing *d* or *f* electrons, the linearization error is rather important such that it may be necessary to add HDLO to the basis set for reasonably converged results. As already shown in Ref. [11], Ce is the worst case of all those we have considered since the error (without HDLO) in the lattice constant with $R_{MT} \sim 3$ Bohr is of the order of 0.1 Bohr. However, the use of HDLO removes nearly 100% of this error.

Therefore, the use of HDLO is recommended for atoms with *d* or *f* electrons in the valence (i.e., transition-metal, rare-earth and actinide atoms) if MT spheres with R_{MT} larger than 2.5 Bohr are used. However, we also observed that HDLO should be added only for the relevant angular momentum (*d* or *f*) in order to avoid problems like linear dependency or the appearance or ghost bands. For small MT spheres, the linearization error is small enough to be neglected and furthermore, HDLO may eventually lead to problems as shown in the case of the CO molecule. Concerning unoccupied states that are not too high in energy (below ∼10 eV), HDLO improve their descriptions, therefore the use of HDLO is recommended for the calculation of optical properties. For very high-lying unoccupied states, only the use of HELO set at the corresponding energies can be used to improve the description of these states. Actually, HELO can also be as efficient as HDLO for the occupied states, however it is maybe less obvious at which energy they should be set, while HDLO are set at the same energy as the parent basis set which makes their use more straightforward.

Acknowledgments

This work was supported by the project SFB-F41 (ViCoM) of the Austrian Science Fund. We are grateful to Gregor Michalicek and John Kay Dewhurst for very useful discussions.

References

[1] P. Hohenberg, W. Kohn, Phys. Rev. 136 (1964) B864–B871. http://dx.doi.org/10.1103/PhysRev.136.B864.
[2] W. Kohn, L.J. Sham, Phys. Rev. 140 (1965) A1133–A1138. http://dx.doi.org/10.1103/PhysRev.140.A1133.
[3] S. Kümmel, L. Kronik, Rev. Modern Phys. 80 (2008) 3–60. http://dx.doi.org/10.1103/RevModPhys.80.3.
[4] A.J. Cohen, P. Mori-Sánchez, W. Yang, Chem. Rev. 112 (1) (2012) 289–320. http://dx.doi.org/10.1021/cr200107z.
[5] R.M. Martin, Electronic Structure: Basic Theory and Practical Methods, Cambridge University Press, 2004.
[6] J.C. Slater, Phys. Rev. 51 (1937) 846–851. http://dx.doi.org/10.1103/PhysRev.51.846.
[7] D.J. Singh, L. Nordström, Planewaves, Pseudopotentials, and the LAPW Method, second ed., Springer, 2005.
[8] O.K. Andersen, Phys. Rev. B 12 (1975) 3060–3083. http://dx.doi.org/10.1103/PhysRevB.12.3060.
[9] E.E. Krasovskii, V.V. Nemoshkalenko, V.N. Antonov, Z. Phys. B 91 (4) (1993) 463–466. http://dx.doi.org/10.1007/BF01316824.
[10] C. Friedrich, A. Schindlmayr, S. Blügel, T. Kotani, Phys. Rev. B 74 (2006) 045104. http://dx.doi.org/10.1103/PhysRevB.74.045104.
[11] G. Michalicek, M. Betzinger, C. Friedrich, S. Blügel, Comput. Phys. Comm. 184 (12) (2013) 2670–2679. http://dx.doi.org/10.1016/j.cpc.2013.07.002.
[12] L. Smrčka, Czech. J. Phys. B 34 (7) (1984) 694–704. http://dx.doi.org/10.1007/BF01589865.
[13] J. Petrů, L. Smrčka, Czech. J. Phys. B 35 (1) (1985) 62–71. http://dx.doi.org/10.1007/BF01590276.
[14] D. Singh, Phys. Rev. B 43 (1991) 6388–6392. http://dx.doi.org/10.1103/PhysRevB.43.6388.
[15] P. Blaha, K. Schwarz, P. Sorantin, Comput. Phys. Comm. 59 (2) (1990) 399–415. http://dx.doi.org/10.1016/0010-4655(90)90187-6.
[16] D. Singh, H. Krakauer, Phys. Rev. B 43 (1991) 1441–1445. http://dx.doi.org/10.1103/PhysRevB.43.1441.
[17] E.E. Krasovskii, A.N. Yaresko, V.N. Antonov, J. Electron Spectrosc. Relat. Phenom. 68 (1994) 157–166. http://dx.doi.org/10.1016/0368-2048(94)02113-9.
[18] E.E. Krasovskii, W. Schattke, Solid State Commun. 93 (9) (1995) 775–779. http://dx.doi.org/10.1016/0038-1098(94)00730-6.
[19] E.E. Krasovskii, Phys. Rev. B 56 (1997) 12866–12873. http://dx.doi.org/10.1103/PhysRevB.56.12866.
[20] M. Betzinger, C. Friedrich, S. Blügel, A. Görling, Phys. Rev. B 83 (2011) 045105. http://dx.doi.org/10.1103/PhysRevB.83.045105.
[21] C. Friedrich, M.C. Müller, S. Blügel, Phys. Rev. B 83 (2011) 081101. http://dx.doi.org/10.1103/PhysRevB.83.081101.
[22] H. Jiang, P. Blaha, Phys. Rev. B 93 (2016) 115203. http://dx.doi.org/10.1103/PhysRevB.93.115203.
[23] D. Nabok, A. Gulans, C. Draxl, Phys. Rev. B 94 (2016) 035118. http://dx.doi.org/10.1103/PhysRevB.94.035118.
[24] R. Laskowski, P. Blaha, Phys. Rev. B 85 (2012) 035132. http://dx.doi.org/10.1103/PhysRevB.85.035132.
[25] E. Sjöstedt, L. Nordström, D.J Singh, Solid State Commun. 114 (1) (2000) 15–20. http://dx.doi.org/10.1016/S0038-1098(99)00577-3.
[26] G.K.H. Madsen, P. Blaha, K. Schwarz, E. Sjöstedt, L. Nordström, Phys. Rev. B 64 (2001) 195134. http://dx.doi.org/10.1103/PhysRevB.64.195134.
[27] P. Blaha, K. Schwarz, G.K.H. Madsen, D. Kvasnicka, J. Luitz, WIEN2K: An Augmented Plane Wave plus Local Orbitals Program for Calculating Crystal Properties, Vienna University of Technology, Austria, 2001.
[28] http://www.flapw.de.
[29] A. Gulans, S. Kontur, C. Meisenbichler, D. Nabok, P. Pavone, S. Rigamonti, S. Sagmeister, U. Werner, C. Draxl, J. Phys.: Condens. Matter 26 (36) (2014) 363202. http://dx.doi.org/10.1088/0953-8984/26/36/363202.
[30] J.P. Perdew, Y. Wang, Phys. Rev. B 45 (23) (1992) 13244–13249. http://dx.doi.org/10.1103/PhysRevB.45.13244.
[31] P. Blaha, K. Schwarz, P.H. Dederichs, Phys. Rev. B 37 (1988) 2792–2796. http://dx.doi.org/10.1103/PhysRevB.37.2792.